

15 **Abstract**

16 Background

17 Plasmids are major drivers of horizontal gene transfer (HGT), playing a central role in
18 disseminating antimicrobial resistance in water resource recovery facilities (WRRFs). Most
19 studies have focused on model or clinical plasmids in simplified settings, leaving their *in situ*
20 dynamics in complex environmental communities poorly understood. To address this gap, we
21 applied Hi-C metagenomic sequencing to systematically resolve plasmid–host associations and
22 evaluate how environmental and operational factors influence plasmid persistence and host range
23 across treatment stages and geographic regions in municipal WRRFs.

24 Results

25 We identified 944 plasmid clusters across influent, activated sludge, and effluent samples from
26 three WRRFs located in three U.S. states, revealing distinct plasmid distribution patterns and
27 plasmid-host associations across facilities and treatment stages. While overall bacterial
28 community composition remained relatively stable across treatment stages, plasmid-host
29 interactions varied, indicating that environmental conditions and treatment processes influenced
30 plasmid retention and transfer. Plasmids in influent and activated sludge exhibited broader host
31 ranges relative to effluent, where, plasmids were associated with a narrower set of bacterial
32 hosts, likely reflecting the impacts of disinfection. Notably, certain plasmids persisted across
33 treatment stages but exhibited substantial shifts in their associated bacterial hosts. Key taxa such
34 as *Burkholderiaceae* and *Rhodocyclaceae* remained abundant throughout, indicating that shifts in
35 plasmid-host associations were not solely driven by community turnover, but also suggesting

36 HGT. Supporting this, functional profiling of effluent plasmids revealed enrichment in
37 conjugation-related genes and virulence factors, including oxidative stress resistance, which may
38 facilitate plasmid persistence and dissemination.

39 Conclusions

40 Our findings reveal that while wastewater microbial communities are diverse, plasmid-associated
41 hosts are restricted to a few dominant bacterial families. Plasmid host range consistently narrows
42 across treatment stages, reflecting the effectiveness of WRRFs in limiting plasmid persistence.
43 However, shifts in host associations among highly similar plasmid clusters suggest potential
44 HGT events. These results highlight the role of specific bacterial groups in plasmid
45 dissemination and underscore the need for future studies to identify keystone taxa and
46 mechanisms driving plasmid stability in complex microbial communities.

47 Keywords

48 Plasmid-host associations; Water resource recovery facilities; Hi-C sequencing; Plasmid
49 retention; Shotgun metagenomics

50 Background

51 Plasmids are extrachromosomal genetic elements that facilitate bacterial adaptation and
52 evolution by mediating horizontal gene transfer (HGT) [1–3]. These mobile genetic elements
53 contribute to the dissemination of antimicrobial resistance (AMR), virulence factors, and
54 metabolic capabilities, significantly shaping the function and dynamics of microbial
55 communities [4–6]. While plasmid biology has been extensively studied under controlled

56 laboratory conditions, the mechanisms governing plasmid persistence, such as conjugative
57 transfer, fitness impacts, selective pressures, interspecies competition, remain to be assessed in
58 complex environmental microbial communities [7–9]. Distinguishing between these mechanisms
59 in representative environmental systems is critical for advancing our understanding of plasmid-
60 host ecology.

61 Water resource recovery facilities (WRRFs) act as critical interfaces between the built and
62 natural environment, facilitating the exchange and dissemination of genetic material, including
63 AMR genes [9,10]. Biological treatment systems like activated sludge provide ideal conditions
64 for HGT and the spread of adaptive traits due to high microbial densities, abundant biofilms, and
65 active microbial metabolism [11–13]. Broad-host-range plasmids are key drivers of this process,
66 transferring between diverse microbial hosts and mobilizing otherwise non-mobilizable
67 plasmids, thereby accelerating the spread of AMR [6,14,15]. Although disinfection processes
68 inactivate bacteria in wastewater effluents, they may not fully eliminate plasmid-carrying
69 bacteria or extracellular DNA, allowing AMR genes to persist [16,17]. Residual plasmids in
70 effluent have been reported as a concern, as they may contribute to the reintroduction of
71 resistance genes into natural ecosystems, where they could be acquired by environmental or
72 opportunistic pathogens [10]. Understanding plasmid persistence throughout treatment processes
73 is crucial for assessing AMR risks and developing strategies to mitigate their dissemination from
74 WRRFs to environmental microbial communities.

75 Despite advances in sequencing technologies, tracking plasmid dissemination and host range is
76 methodologically challenging. Laboratory-based approaches, such as synthetic plasmid systems
77 and culture-based conjugation assays, often rely on well-characterized, culturable hosts and

78 controlled conditions, failing to capture the complexity of natural microbial ecosystems [18–20].
79 While emerging metagenomic approaches, including high-throughput single-cell sequencing, can
80 be used to reveal host-MGE associations, they are limited by incomplete genome recovery,
81 amplification biases, and insufficient sequencing depth, hindering the reconstruction of complete
82 plasmid sequences and transmission networks [21,22].

83 Chromosome conformation capture sequencing, like Hi-C, preserves spatial interactions between
84 plasmids and their hosts within intact microbial communities. This provides key ecological
85 context for understanding plasmid dissemination in microbial communities [23–25]. Unlike
86 single-cell sequencing, which isolates individual cells and may miss community interactions, Hi-
87 C maintains *in situ* associations, enabling a more comprehensive reconstruction of plasmid-host
88 networks. This capability is particularly valuable in complex environments such as WRRFs,
89 where plasmids circulate among diverse taxa. Hi-C studies have inferred plasmid-host
90 associations using either contig-level or bin-level data [24,25]. Contig-level analyses are highly
91 sensitive, detecting links even for fragmented and low-abundance plasmids, but the loss of
92 broader genomic context can inflate apparent host ranges. Bin-level analyses retain genomic
93 context and improve host-range estimates, but they are more vulnerable to Hi-C noise.

94 Artefactual links from contig ends or IS elements, as well as incomplete binning, can result in
95 host misassignments [26]. In this study, to track plasmids from influent to effluent and examine
96 their genetic context, we adapted a recent Hi-C-based plasmid clustering framework [23], and
97 implemented a graph-based approach to group plasmid contigs into putative plasmid units with
98 stringent linkage thresholds, aiming to provide a conservative, context-preserving basis for
99 plasmid-host associations.

100 In this study, we applied Hi-C metagenomics and performed plasmid clustering to systematically
101 track plasmid-host linkages across multiple unit processes within WRRFs in three U.S. states.
102 Our objectives were to: (1) characterize the distribution of plasmids across treatment stages, (2)
103 unravel plasmid-host associations with improved resolution of plasmid genetic context (e.g.,
104 encoded functions, plasmid mobility), and (3) identify key bacterial taxa that function as plasmid
105 reservoirs. This study enhances our understanding of plasmid persistence and transmission in
106 WRRFs by offering new insights into their microbial ecology.

107 **Methods**

108 Sample Collection and Concentration

109 Wastewater samples were collected weekly from three U.S. WRRFs in States A, B, and C, three
110 times over a month. Primary influent was obtained as 24-hour composite samples (States A and
111 B) or via grab sampling (State C). AS samples were collected via grab sampling from all sites,
112 and effluent was grab-sampled after chlorination in States A and B, and combined
113 UV/chlorination in State C. Effluent from State A underwent tertiary filtration to remove fine
114 solids prior to chlorination. Samples from States A and C were shipped on ice to State B and
115 stored at 4°C until processing. State A does not employ primary clarification; instead, influent
116 undergoes preliminary screening and flows directly into the activated sludge process. State C
117 operated a five-stage Bardenpho system with filtration and UV disinfection, while States A and
118 B used high-purity oxygen activated sludge systems. All WRRFs discharged to local surface
119 waters. Influent and AS samples were aliquoted into 50 mL and 2.0 mL tubes, respectively,
120 centrifuged at $12,000 \times g$ for 10 min at 4°C, and pellets stored at 4°C. Effluent (500 mL) was
121 centrifuged at $3,500 \times g$ for 30 min, pooled, recentrifuged, and pellets stored at 4°C. All samples

122 were processed in duplicate: one replicate for Hi-C sequencing and the other for metagenomic
123 DNA extraction.

124 Hi-C sample preparation

125 One replicate per sample (by site, type, and date) was processed using the ProxiMeta™ Hi-C Kit
126 (Phase Genomics, Seattle, WA, USA) following protocol v4.5.4, with modified crosslinking.
127 Briefly, samples were incubated with 10 mL of chilled 1× PBS containing 1% formaldehyde for
128 10 min at room temperature, then quenched with 527 μL of 2.5 M glycine for 5 min. After a
129 10 min incubation on ice with agitation, samples were centrifuged at 3,500 × g for 10 min at 4°C,
130 washed twice with cold 1× PBS, and resuspended in 1.0 mL PBS. A final spin at 800 × g for
131 5 min at 4°C was performed before storing the pellets at -80°C. Remaining steps followed the
132 manufacturer's instructions.

133 DNA extraction and sequencing

134 Genomic DNA was extracted from pellet replicates using the Maxwell® RSC 48 system and
135 Blood DNA Kit (Promega, Madison, WI, USA), with modified lysis to address solids in
136 wastewater. Pellets were combined with 0.5 g zirconia beads (BioSpec) and 300 μL lysis buffer,
137 bead-beaten at 2,400 RPM for 2 minutes, and centrifuged at 15,000 × g for 5 minutes. The
138 supernatant (200 μL) was collected. This process was repeated twice with fresh lysis buffer,
139 yielding 600 μL total lysate. Proteinase K (60 μL) was added, followed by incubation at 56°C for
140 30 minutes. DNA extracts were submitted to the Oklahoma Medical Research Foundation
141 Clinical Genomics Core (Oklahoma City, OK) for library preparation using the Watchmaker
142 DNA Library Prep Kit (Watchmaker Genomics, Boulder, CO) and sequenced on an Illumina

143 NovaSeq X Plus (Illumina, San Diego, CA) to a depth of 100 million reads per sample. Indexed
144 Hi-C libraries were pooled and sequenced separately at the Duke Sequencing and Genomic
145 Technologies Core (Durham, NC) under the same platform and read depth.

146 Shotgun metagenomic and Hi-C data analysis

147 Shotgun reads were quality-filtered and adapter-trimmed using BBDuk (BBTools, Joint Genome
148 Institute) with the following parameters: $k=23$, $ktrim=r$, $mink=12$, $hdist=1$, $minlength=50$, $-tpe$,
149 $-tbo$ for adapter removal, and $qtrim=rl$, $trimq=10$, $chastityfilter=True$ for low-quality base
150 trimming. Trimmed reads were assembled using MEGAHIT with default parameters [27].
151 Shotgun and Hi-C reads were mapped to the assemblies using Bowtie2 and processed with
152 Samtools, while Hi-C-specific alignments were performed using BWA-MEM [28–30]. Genome
153 binning was conducted with MetaCC, which uses Hi-C contact frequencies to cluster contigs
154 [31]. In total, binning across all samples recovered 988 metagenome-assembled genomes
155 (MAGs) for State A, 1,475 MAGs for State B, and 882 MAGs for State C. Contact matrices were
156 derived from Hi-C BAM files using the custom script *bam2links.py*, which quantifies linkage
157 between contigs, as described by Press *et al* [32]. MAGs were annotated using Prokka,
158 taxonomically classified with GTDB-Tk, and assessed for quality using CheckM [33–35]. While
159 MAGs typically represent near-complete genomes of individual organisms, the quality of most
160 MAGs in this study, as indicated by genome size and completeness estimates from CheckM, did
161 not support this assumption. Accordingly, we interpret MAGs more broadly as genomes or
162 genome fragments from closely related strains within a species. Plasmid contigs were identified
163 and characterized using geNomad using the *end-to-end* command [36].

164 Plasmid clusters identification and functional annotation

165 Putative plasmid contigs were identified using a Hi-C-based approach adapted from Risely *et*
166 *al.*[23]. First, protein-coding genes were predicted from assembled contigs using Prodigal in
167 metagenomic mode (-p meta) [37]. To minimize false-positive associations driven by mobile
168 elements, contigs encoding transposases or insertion sequences (IS elements) were excluded.
169 These were identified via BLASTp searches (e-value < 0.01) against curated transposase
170 databases from ISfinder and the Tn3 Transposon Finder [38,39]. Contigs predicted to be
171 plasmid-derived using geNomad were retained only if they exhibited strong linkage (≥ 15 Hi-C
172 contacts) to at least one other plasmid contig, reflecting the assumption that genuine plasmids
173 tend to co-occur stably in Hi-C networks. While this filtering may exclude small or non-
174 transferable plasmids, it helps enrich for conjugative or mobilizable elements that are more
175 ecologically relevant to HGT, as noted by Risely *et al.* [23]. Graph-based clustering of the
176 retained contigs was then performed using the Walktrap algorithm (igraph::walktrap.community,
177 step length = 10) [40], yielding a total of 944 plasmid clusters (Supplementary Fig. 1). Plasmid-
178 cluster lengths ranged from 2,051 to 140,087 bp and were largely comparable across states
179 (Supplementary Fig. 2). Lengths fall within reported ranges for natural plasmids [41,42]. Hi-C
180 contact data were then integrated to identify host associations, revealing 289 plasmid clusters
181 linked to at least one metagenome-assembled genome (MAG). These host-linked clusters were
182 used in subsequent analyses. Hi-C contact counts were normalized for differences in host
183 abundance and plasmid size, following the general approach of Risely *et al.* and Stalder *et al.*
184 [23,25]. Specifically, for each MAG-plasmid pair, the raw Hi-C contact value was scaled by the
185 average shotgun-derived MAG read count across all MAGs in the dataset relative to the read
186 count for that MAG, and by the average plasmid cluster length across all plasmid clusters
187 relative to the length of the individual plasmid cluster. This correction reduces detection biases

188 introduced by variation in microbial abundance and plasmid size, enabling more comparable
189 contact frequencies across samples (Supplementary Table 1).

190

191 Functional annotation was performed to target plasmid mobility, virulence factors, and AMR
192 genes. MOB-suite (<https://github.com/phac-nml/mob-suite>) was used to classify plasmid clusters
193 based on mobility-associated genes, including relaxases, origin-of-transfer (oriT) sites, and
194 mating pair formation (MPF) systems [43]. Virulence factors were identified using ABRicate
195 (<https://github.com/tseemann/abricate>) with the Virulence Factors Database (VFDB), retaining
196 hits that met a minimum sequence identity of $\geq 75\%$ and coverage of $\geq 70\%$ [44]. AMR genes
197 were detected using AMRFinderPlus, which identifies resistance determinants based on curated
198 sequence models and HMM-based classification [45].

199 Analysis of plasmid-host dynamics and plasmid persistence

200 To compare the total and plasmid-associated microbial communities, Hi-C and shotgun
201 metagenomic data were aggregated across three weekly samples per stage. Relative abundances
202 of bacterial families were used to assess community structure via non-metric multidimensional
203 scaling (NMDS) based on Bray-Curtis dissimilarity (`vegan::metaMDS`) and evaluated by state
204 and treatment stage using PERMANOVA (`vegan::adonis2`) [46]. Alpha diversity (Shannon
205 index) was computed with `vegan::diversity`, and differences across groups were tested using
206 Kruskal-Wallis and pairwise Wilcoxon tests (`ggpubr::stat_compare_means`) [47,48].

207 The number of plasmid clusters associated with each MAG and the host range of each plasmid
208 cluster were quantified and compared across states. Plasmid-host bipartite networks were
209 constructed from normalized Hi-C linkage data, retaining only associations with values ≥ 0.01 to

210 exclude spurious contacts [25]. To evaluate plasmid persistence across wastewater treatment, we
211 identified plasmid clusters that were highly similar ($\geq 80\%$ nucleotide identity) and detected
212 across all three treatment stages. Sequence similarity between clusters was assessed using
213 BLAST, and persistent plasmids were defined as those present in all three stages within a
214 facility. Due to the fragmented nature of metagenomic assemblies and inherent variation in
215 plasmid sizes, we did not apply a strict alignment length cutoff. While this approach may capture
216 shared modular elements rather than entire plasmid sequences, it provides a conservative
217 estimate of plasmid-associated sequence continuity across stages.

218 **Results**

219 **Hi-C–derived plasmid-associated communities exhibit greater variability across states than** 220 **total microbial communities.**

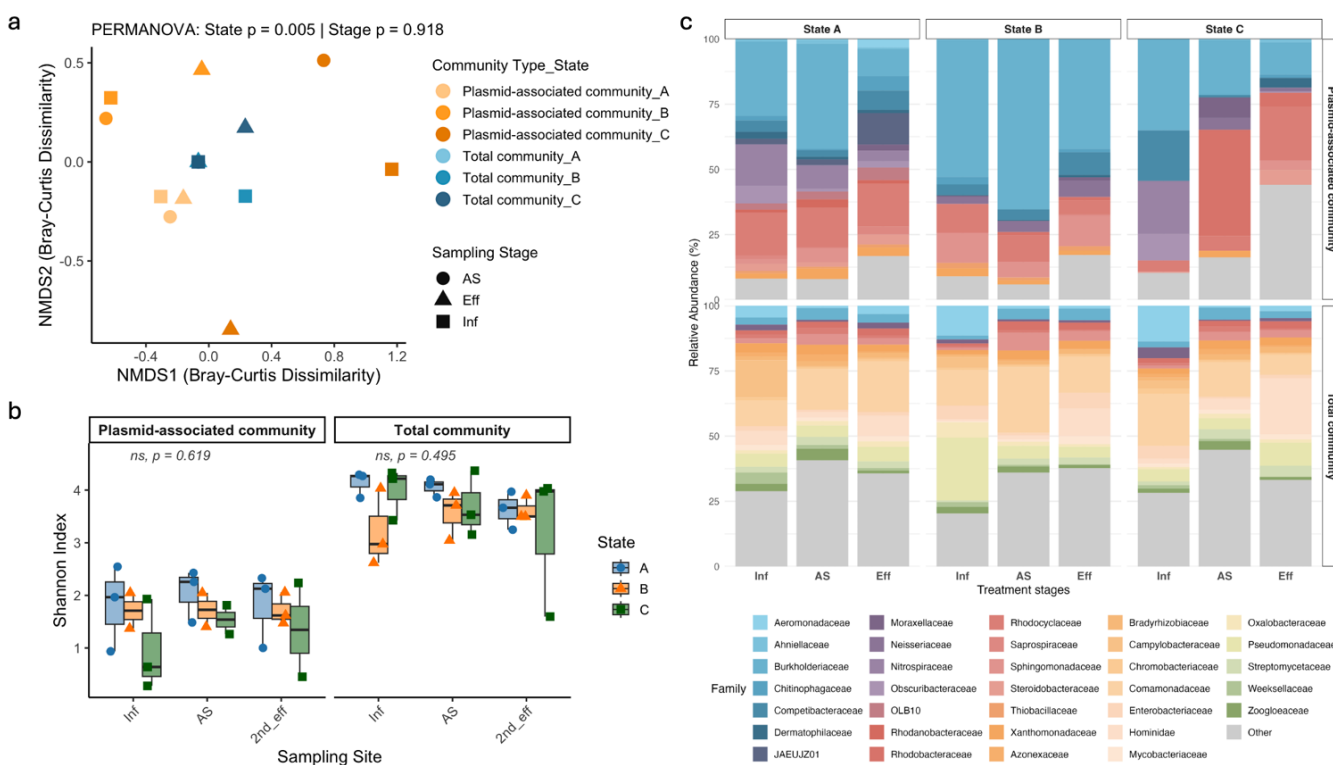
221 We began by comparing microbial and plasmid-associated communities across three states (A,
222 B, and C) and three wastewater treatment stages: influent (Inf), activated sludge (AS), and
223 effluent (Eff). Both were assessed at the MAG level (GTDB-Tk taxonomy), with
224 plasmid-associated profiles including only MAGs linked to plasmids via Hi-C contacts. For each
225 state and stage, the three weekly samples were combined and re-normalizing to produce a single
226 representative community profile for that stage. Community-level variation was assessed using
227 non-metric multidimensional scaling (NMDS) based on Bray–Curtis dissimilarities (Fig. 1a).
228 Both shotgun and Hi-C–derived plasmid-host datasets revealed state-specific clustering of the
229 microbial communities, with samples from the same state appearing more similar than those
230 from different states. Furthermore, the Hi-C–based plasmid-associated communities showed
231 more distant separation across states as compared to total communities. PERMANOVA analysis

232 confirmed that geographical location (state) significantly influenced community composition (p
233 = 0.015 for shotgun; $p = 0.004$ for Hi-C), whereas treatment stage had no significant effect ($p >$
234 0.9). Notably, the effect size was larger in the Hi-C dataset ($R^2 = 0.508$) than in the shotgun data
235 ($R^2 = 0.364$), indicating that plasmid-associated communities were more variable across states
236 than the total communities. This finding suggests that plasmid-host associations are more
237 sensitive to differences in influent sources or treatment technologies across states than the overall
238 microbial community structure.

239 We next assessed alpha diversity using the Shannon index (Fig. 1b). Across all states and stages,
240 total communities via shotgun metagenomes exhibited consistently higher diversity as compared
241 to Hi-C-derived plasmid-associated communities. This reflects that plasmid-associated taxa
242 represent only a subset of the overall microbial community. No significant differences in alpha
243 diversity were observed across stages or states ($p > 0.05$), indicating that the diversity of total
244 and plasmid-associated communities was relatively stable both across the treatment systems and
245 across states. Additionally, Hi-C crosslinking may not capture all plasmid-bearing taxa, which
246 could further contribute to lower observed diversity in the plasmid-associated fraction.

247 To better understand these differences in community composition between the total and plasmid-
248 associated communities, we examined the taxonomic profiles derived from both shotgun and Hi-
249 C data (Fig. 1c). We found that the dominant taxa were distinct between the total and plasmid-
250 host communities. Specifically, shotgun metagenomes were dominated by *Comamonadaceae*
251 (15.2% on average), followed by *Hominidae* (7.2%), *Pseudomonadaceae* (6.4%),
252 *Aeromonadaceae* (4.6%), and *Burkholderiaceae* (4.4%). In contrast, the Hi-C-linked plasmid-
253 associated taxa displayed a markedly narrower taxonomic spectrum. The dominant families in

254 these profiles included *Burkholderiaceae* (34.3%), *UBA10799* (18.0%, within *Actinomycetes*),
 255 *Neisseriaceae* (15.3%), *Nitrospiraceae* (14.2%), and *Rhodocyclaceae* (12.6%). These findings
 256 highlight that the families that were most abundant in the overall community may not play major
 257 roles in plasmid retention. Instead, plasmid dissemination appears to be facilitated by a distinct
 258 set of bacterial families.



259

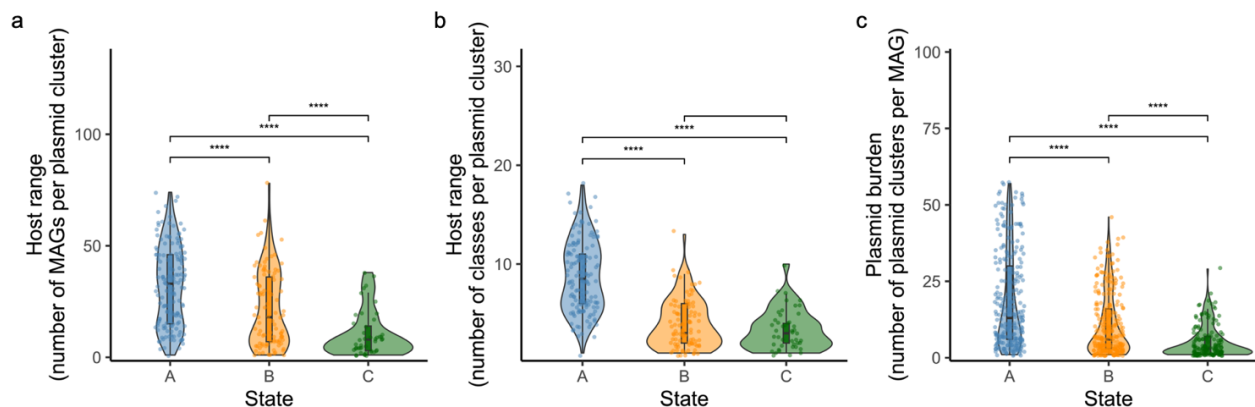
260 **Fig. 1 Microbial community composition, plasmid-associated taxa, and diversity patterns**
 261 **across states and wastewater treatment stages.** (a) Non-metric multidimensional scaling
 262 (NMDS) plots based on Bray–Curtis dissimilarities show sample clustering by state for Hi-C-
 263 derived plasmid-associated taxa and shotgun-derived total bacterial communities.
 264 PERMANOVA revealed significant differences across states (Hi-C: $p = 0.004$, $R^2 = 0.508$;
 265 Shotgun: $p = 0.015$, $R^2 = 0.364$), while treatment stage had no significant effect ($p > 0.9$). (b)

266 Shannon diversity (alpha diversity) of plasmid-associated (Hi-C) and total (shotgun)
267 communities across samples. Shotgun data consistently showed higher diversity than Hi-C
268 profiles, with no significant differences across states or stages ($p > 0.05$). (c) Relative abundance
269 of the top 20 bacterial families in (top) plasmid-associated communities identified via Hi-C
270 linkages to plasmid contigs and (bottom) total communities based on shotgun metagenomes.
271 Taxonomic classifications are shown at the family level.

272 **Broader host range and higher plasmid prevalence in the State A WRRF may enhance**
273 **HGT potential.**

274 To evaluate plasmid dissemination dynamics, we quantified: (1) plasmid host range, defined as
275 either the number of unique metagenome-assembled genomes (MAGs; individual genome bins)
276 or the number of distinct bacterial classes (taxonomic groups) associated with each plasmid
277 cluster, and (2) plasmid burden, defined as the number of unique plasmid clusters associated with
278 each MAG. Plasmids in the State A WRRF exhibited the broadest host ranges, averaging $8.8 \pm$
279 0.29 bacterial classes and 32.2 ± 1.48 MAGs per cluster, with some clusters linked to as many as
280 18 classes and 74 MAGs (Fig. 2a-b). In contrast, plasmids from the State B and State C WRRFs
281 had lower host ranges, averaging 3.9 ± 0.25 and 3.4 ± 0.30 classes, respectively. These
282 differences were statistically significant ($p < 0.0001$, Wilcoxon rank-sum test with Benjamini–
283 Hochberg adjustment). Plasmid burden per MAG showed a similar trend (Fig. 2c;
284 Supplementary Fig. 3): MAGs in the State A WRRF carried on average 18.6 ± 0.98 plasmid
285 clusters (max = 57), compared to 10.5 ± 0.62 in State B (max = 46) and 5.1 ± 0.41 in State C
286 (max = 29). These differences were also significant ($p < 0.0001$, Wilcoxon rank-sum test with
287 Benjamini–Hochberg adjustment), indicating a higher plasmid load in the microbial community

288 of the State A WRRF. The co-occurrence of broader plasmid dissemination and elevated plasmid
289 burden may reflect enhanced HGT potential in the microbial communities of this facility.



290

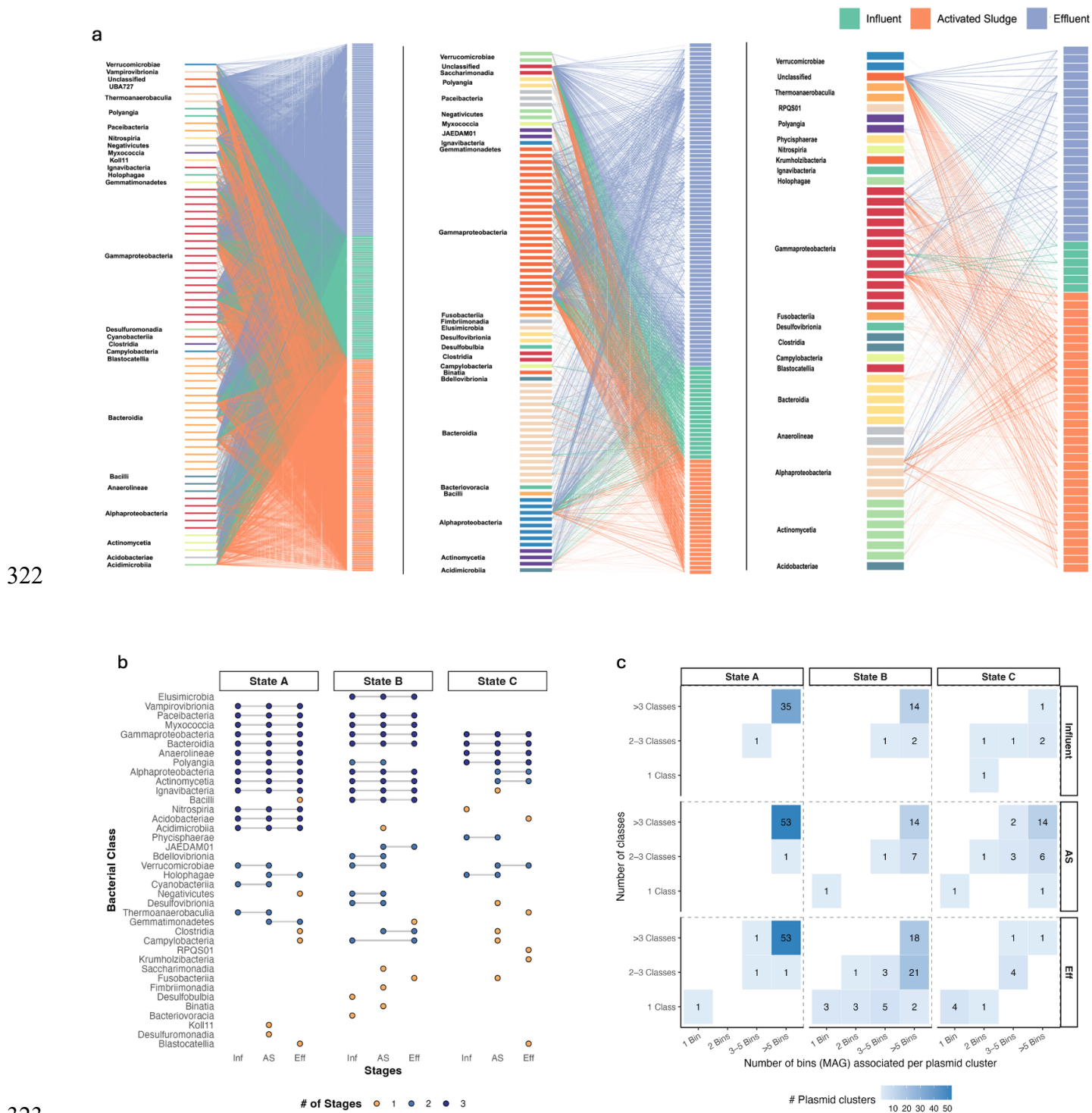
291 **Fig. 2 Plasmid-host associations and dissemination metrics across wastewater treatment**

292 **samples.** (a-b) Violin plots showing the distribution of plasmid host range, defined as the
293 number of MAGs (a) and the number of bacterial classes (b) associated with each plasmid cluster
294 in States A, B, and C. (c) Violin plot showing plasmid burden per MAG across states. For all
295 panels, pairwise differences between states were evaluated using the unpaired Wilcoxon rank-
296 sum test with Benjamini–Hochberg adjustment; significance levels are indicated by asterisks: $p <$
297 0.05 (*), $p < 0.01$ (**), $p < 0.001$ (***) and $p < 0.0001$ (****).

298 To further investigate WRRF-specific differences in plasmid-host interaction structure, we
299 constructed bipartite networks linking plasmid clusters to bacterial host classes (Fig. 3a). The
300 number of host-linked plasmid clusters varied among facilities (State A WRRF: 148; State B
301 WRRF: 96; State C WRRF: 45), which may contribute to differences in apparent network
302 complexity. Despite this, these networks revealed marked contrasts in connectivity across states.
303 The State A WRRF showed a highly interconnected network, with many plasmid clusters linked
304 to multiple host classes, indicating extensive cross-lineage dissemination. The State B WRRF

305 displayed a more modular structure, with most plasmid clusters limited to
306 *Gammaproteobacteria*, *Bacteroidia* and *Alphaproteobacteria*. The State C WRRF displayed
307 sparse connectivity, suggesting a narrower host range and limited plasmid mobility within the
308 microbial community.

309 To explore the observed differences, we analyzed the persistence of plasmid-host associations
310 across treatment stages within each state (Fig. 3b). The State A WRRF retained a diverse and
311 stable set of host classes across all stages, with many associations maintained from influent to
312 effluent. In contrast, the State B and State C WRRFs showed more stage-specific patterns, with
313 fewer host classes shared between stages, indicating lower persistence of plasmid-host
314 associations. We also quantified the occurrence of broadly distributed plasmids (e.g., ≥ 3 bacterial
315 classes, ≥ 5 MAGs) across treatment stages (Fig. 3c). While such broad host ranges are relatively
316 uncommon, cross-class transfer has been documented experimentally for promiscuous
317 conjugative plasmids, including IncP-1, IncU, and IncW groups [49,50]. The State A WRRF
318 consistently carried more broadly distributed plasmids, whereas most plasmids in the State C
319 WRRF were confined to a single host class and a small number of MAGs. These findings
320 suggest that the greater network connectivity observed in the State A WRRF is driven by broader
321 plasmid host ranges and higher plasmid prevalence, reflecting greater HGT potential.



322

323

324 **Fig. 3 WRRF-specific patterns of plasmid-host association structure, host distribution**

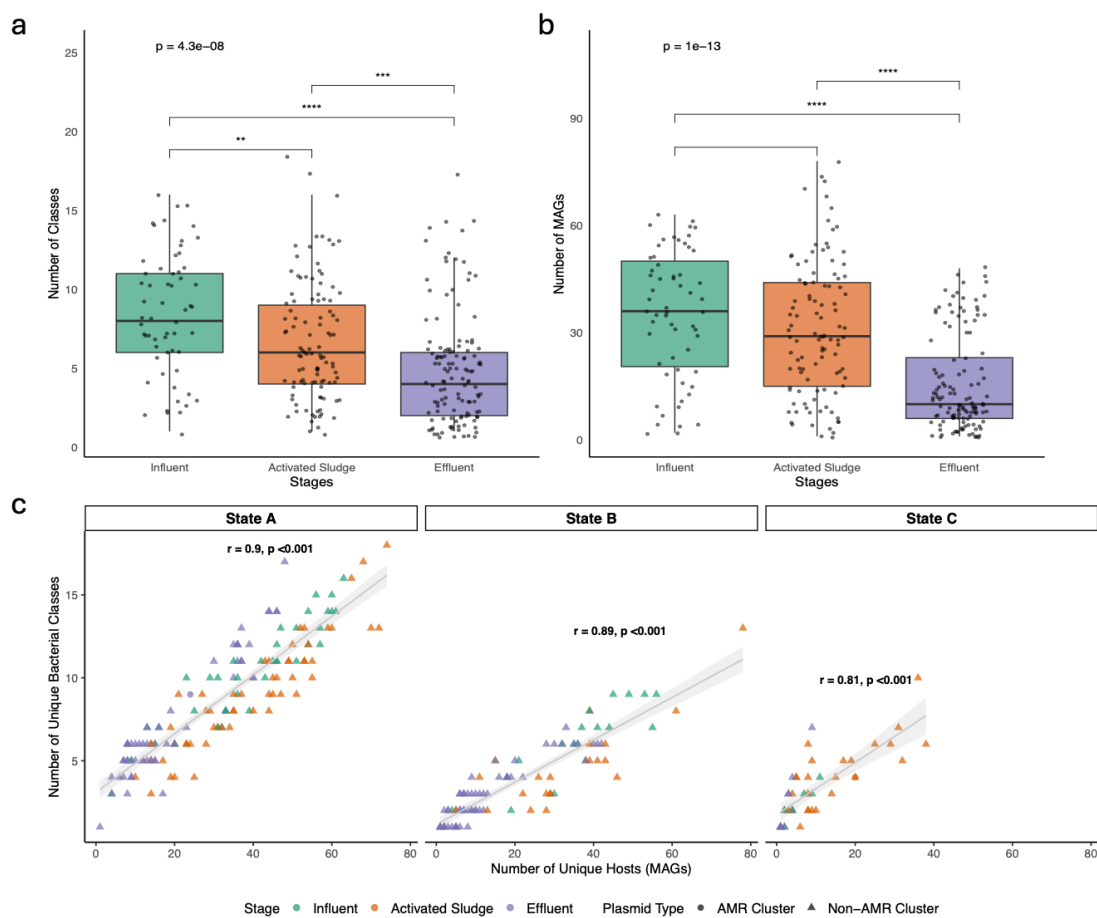
325 **across stages, and plasmid dissemination metrics. (a) Bipartite networks linking plasmid**

326 clusters (right columns, colored by treatment stages) to bacterial host families (left columns,
327 colored by taxonomic class) in the State A, State B, and State C WRRFs. Edges represent
328 plasmid–host associations inferred from Hi-C linkages. (b) Presence–absence matrix of plasmid-
329 carrying bacterial classes across treatment stages. Each dot represents the detection of a given
330 plasmid-carrying bacterial class. Dot color indicates persistence across stages: dark blue =
331 detected in all three stages, light blue = detected in two stages, and yellow = detected in only one
332 stage. (c) Heatmaps showing the number of plasmid clusters binned by host burden (i.e., the
333 number of associated MAGs) and host range (i.e., the number of associated bacterial classes and
334 bins) across treatment stages in each WRRF.

335 **Plasmid hosts shifted across treatment stages**

336 We next investigated plasmid cluster distribution across treatment stages by quantifying their
337 host range, defined as the number of associated MAGs and bacterial classes. Host range was
338 calculated within each WRRF, and per-WRRF counts were pooled for stage-level comparisons.
339 Plasmid host range differed significantly between stages: plasmids from influent and AS were
340 associated with more MAGs and classes than those from effluent ($p < 0.01$, Wilcoxon test; Fig.
341 4a-b). WRRF-specific analyses (Supplementary Fig. 4a-b) showed a consistent overall pattern,
342 though the degree of host range reduction from influent to effluent varied, likely reflecting
343 differences in treatment configuration and/or influent composition. This suggests that plasmids
344 with broader host ranges are more common in earlier stages of treatment, while those persisting
345 in the effluent tend to be more host-restricted. Across all states, the number of MAGs per
346 plasmid cluster was strongly correlated with the number of host classes per cluster ($r > 0.81$, $p <$

347 0.001; Fig. 4c), indicating that plasmids associating with more genomes also tend to span greater
348 phylogenetic breadth.



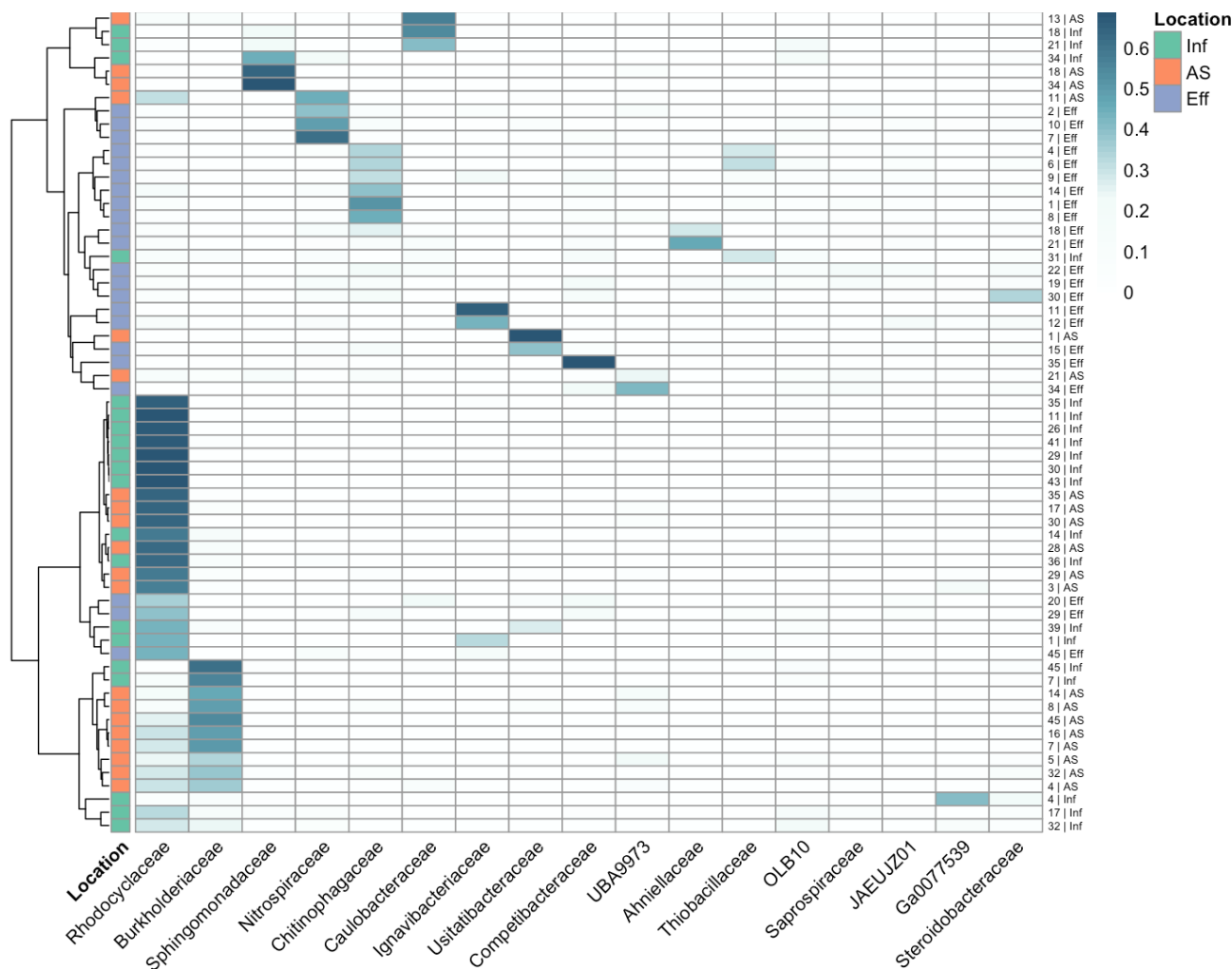
349

350 **Fig. 4 Plasmid host range across wastewater treatment stages.** (a–b) Boxplots showing the
351 distribution of host range metrics across stages: (a) number of unique bacterial classes and (b)
352 number of unique MAGs per plasmid cluster. Asterisks indicate significance levels for pairwise
353 comparisons: $p < 0.05$ (*), $p < 0.01$ (**), $p < 0.001$ (***) and $p < 0.0001$ (****). Dots represent
354 individual clusters; box limits indicate interquartile range, with medians shown as bold lines. (c)
355 Scatter plots showing the relationship between the number of unique MAGs (x-axis) and the
356 number of unique bacterial classes (y-axis) associated with each plasmid cluster in the States A,

357 B, and C WRRFs. Each point represents a plasmid cluster, colored by stage: influent (green), AS
358 (orange), and effluent (purple). Spearman's correlation coefficients (r) are shown for each state,
359 with shaded areas indicating 95% confidence intervals.

360 To assess plasmid persistence across the wastewater treatment process, we then focused on
361 structurally conserved plasmid clusters. Clusters were considered highly similar if they shared
362 $\geq 80\%$ nucleotide identity, representing conserved plasmid backbones. Plasmid clusters were
363 deemed persistent if they were present in all three treatment stages from the same week. This
364 analysis yielded 45 persistent plasmid clusters in the State A WRRF and 135 in the State B
365 WRRF (Supplementary Table 2a-b). No persistent plasmid clusters were detected across multiple
366 stages in the State C WRRF, likely due to limited detection of plasmid clusters in influent
367 samples and their absence in several sampling timepoints, preventing cross-stage comparisons.

368 We next examined whether persistent plasmids maintained stable host associations or shifted
369 hosts across the treatment process. We performed hierarchical clustering based on the host range
370 of the persistent plasmid clusters and found that the plasmid clusters grouped mainly by
371 treatment stage (Fig. 5 shows State A; Supplementary Fig. 5 shows State B). This pattern
372 indicates that persistent plasmids frequently shift host associations between stages, suggesting
373 dynamic host relationships and potential horizontal transfer during treatment. For instance,
374 *Rhodocyclaceae* and *Burkholderiaceae* were frequent plasmid hosts in influent and activated
375 sludge but not in effluent. Notably, their overall relative abundances remained stable across
376 stages (Fig. 1c; Supplementary Fig. 6). This finding suggests that plasmid-host associations are
377 not solely driven by host abundance but may instead reflect selective interactions or
378 compatibility between specific plasmids and hosts in different environmental contexts.



379

380 **Fig. 5 Shifts in host associations of persistent plasmid clusters across treatment stages.**

381 Heatmap for State A (State B in Supplementary Fig. 5). Columns are bacterial host families;

382 rows are persistent plasmid clusters ($\geq 80\%$ sequence identity and detected in influent, activated

383 sludge, and effluent within the same sampling week). Row labels are persistent ID | stage (Inf,

384 AS, Eff). The right-side bar indicates treatment stage. Color intensity represents log-scaled

385 normalized Hi-C contact frequency, reflecting the strength of plasmid-host associations. Rows

386 are clustered by similarity in host-family profiles (y-axis dendrogram).

387 **Mobility potential and virulence content of plasmid clusters**

388 We characterized the mobility potential of plasmid clusters by identifying genes involved in
389 conjugation, including MOB genes and components of the Type IV secretion system (T4SS). A
390 positive relationship was observed between the number of mobility-associated genes (MOB and
391 T4SS) within plasmid clusters and the taxonomic breadth of their associated hosts
392 (Supplementary Fig. 7a). Specifically, genes such as *MOBP*, *MOBQ*, *virB4*, and *trbC* were
393 commonly detected in plasmid clusters linked to diverse host families, including members of
394 *Gammaproteobacteria* (e.g., *Burkholderacace*, *Xanthomonaceae*, *Competitionibactericaea*),
395 *Actinobacteria* (e.g., *Mycobacteriaceae*), and *Bacteroidota* (e.g., *Chitinophageaceae*)
396 (Supplementary Fig. 7b). In addition to conjugation genes, several plasmid clusters carried
397 virulence factors (VFs) involved in oxidative stress defense (*HPI*, *KatG*), membrane remodeling
398 (*PLD*), or resource acquisition (*HasD*). For example, one plasmid cluster from State B co-
399 encoded the oxidative stress gene *HPI* along with multiple conjugation genes (*virB3*, *virB4*,
400 *virB6*, *virB9*) and was linked to diverse host families (Supplementary Fig. 7c). These findings
401 highlight a subset of potentially mobile virulence plasmids with broad host connectivity and
402 provide additional support for the biological relevance and robustness of the identified plasmid
403 clusters.

404 **Discussion**

405 In this study, we evaluated shifts in plasmid-host associations across wastewater treatment stages
406 in multiple states to understand plasmid persistence in complex microbial communities. We
407 achieved this by adopting a recently developed methodology to group plasmid contigs into
408 plasmid clusters. To improve upon contig-based limitations in host assignment and plasmid
409 resolution, we applied a graph-based clustering approach that integrates Hi-C contact data with

410 sequence similarity, grouping contigs into coherent plasmid clusters. This method reduces host
411 association bias and allows for higher-resolution tracking of plasmid distribution and mobility
412 potential across treatment stages using plasmid clusters. We also identified persistent plasmid
413 clusters, defined as structurally conserved plasmid clusters present across all treatment stages,
414 and used this approach to evaluate plasmid host shifts during wastewater treatment.

415 **Plasmid-host associations are selective and constrained to certain bacterial families**

416 Across all WRRFs and treatment stages, plasmid-associated taxa constituted only a narrow
417 subset of the total microbial community, indicating strong host–plasmid selectivity. Certain
418 bacterial families, particularly *Burkholderiaceae*, *Nitrospiraceae*, and *Rhodocyclaceae*, were
419 consistently overrepresented in plasmid-host networks, suggesting their enhanced permissiveness
420 to plasmid acquisition and maintenance. These families harbor traits that likely support plasmid
421 persistence. *Burkholderiaceae* are metabolically versatile and stress-tolerant, capable of
422 producing antifungal compounds and withstanding oxidative stress, facilitating survival in
423 dynamic environments [51,52]. *Nitrospiraceae*, including *Nitrospira marina*, exhibit redox
424 adaptability and flexible energy metabolisms [53], while *Rhodocyclaceae*, such as *Azonexus*, are
425 denitrifiers with broad substrate utilization, commonly found in wastewater systems [54]. These
426 traits may facilitate their role as stable plasmid hosts in dynamic treatment environments.
427 Plasmid persistence also depends on host fitness, conjugation rates, and interspecies competition
428 [55,56]. Together, our findings suggest these families act as key plasmid reservoirs in wastewater
429 microbiomes. Future work should identify and characterize plasmid-host pairs that consistently
430 promote plasmid maintenance to elucidate the ecological and genetic factors stabilizing plasmids
431 in complex communities.

432 **Operational and environmental context modulates plasmid host range and plasmid burden**

433 Despite standardized sampling across treatment stages, plasmid prevalence and host range varied
434 substantially across states. These differences likely reflect variation in operational design,
435 influent characteristics, and environmental conditions. The WRRF in State A, which lacks
436 primary clarification and uses a high-capacity activated sludge system with pure oxygen
437 aeration, exhibited the broadest plasmid host range. This configuration supports high microbial
438 biomass density and sustained aerobic activity, conditions favorable for conjugation and long-
439 term plasmid maintenance [57–59]. Prior studies have shown that aeration and high dissolved
440 oxygen concentrations can enhance plasmid host diversity by shaping microbial communities
441 more permissive to HGT [60–62]. In contrast, the WRRF in State B also employs pure oxygen
442 aeration but includes primary clarification. This step can selectively eliminate non-motile and
443 floc-forming taxa via sedimentation, limiting the introduction of key bacterial groups into the
444 aeration tanks and potentially reducing opportunities for plasmid transfer [63].

445 The WRRF in State C, which operates a five-stage Bardenpho process, exhibited the lowest
446 overall plasmid host range and plasmid burden across stages. The alternating aerobic, anoxic,
447 and anaerobic conditions inherent to this configuration likely impose energetic and regulatory
448 constraints that limit plasmid stability. Previous work suggests that redox fluctuations can impair
449 plasmid retention and horizontal transfer [64,65]. Additionally, frequent redox shifts, elevated
450 biomass turnover, and rapid changes in microbial community composition may impose selective
451 pressure against metabolically costly plasmids, narrowing host range and reducing plasmid
452 permissiveness [66–68]. The relatively small catchment population served by the WRRF in State
453 C may have also contributed to the lower observed diversity of incoming bacterial taxa and

454 plasmids. These findings underscore the combined influence of redox regime and influent source
455 diversity as key drivers of plasmid ecology in WRRFs, shaping both plasmid persistence and
456 dissemination potential.

457 **Host switching and adaptive traits enable plasmid persistence through wastewater** 458 **treatment**

459 Although the overall bacterial community composition remained relatively stable across
460 treatment stages, we observed a significant reduction in plasmid host range from influent to
461 effluent, consistent with strong selective pressures imposed by wastewater treatment [69–71].
462 Persistent plasmids, identified across multiple treatment stages, were frequently associated with
463 different host families at different points in the process. For example, the same plasmid
464 backbones were linked to *Burkholderiaceae* in earlier stages but shifted to families such as
465 *Thiobacillaceae* or *Nitrospiraceae* in the effluent. These shifts in host associations occurred even
466 though the original host families remained abundant, suggesting that plasmid persistence is
467 influenced more by plasmid-host compatibility and environmental selection than by host
468 availability alone.

469 In fact, plasmid clusters spanning influent to effluent often encoded mobilization genes (e.g.,
470 *MOBQ*, *MOBP*, *MOBH*), type IV secretion system components, and adaptive traits such as
471 oxidative stress resistance, membrane repair, and nutrient acquisition functions (Supplementary
472 Fig. 5; Supplementary Table 2). These features likely enhance their ability to transfer and persist
473 under treatment-imposed stressors like redox fluctuations and nutrient limitation. Previous
474 studies similarly found that WRRFs act as ecological filters, favoring mobile and functionally
475 adaptive plasmids while attenuating others [72,73]. For example, core class 1 integron gene

476 cassettes with high resistance potential were found to persist through the treatment process, while
477 others were attenuated, indicating selection against less stable genetic configurations [72].
478 Notably, we did not find any antibiotic resistance genes (ARGs) on persistent plasmids. This is
479 likely because removing transposon- and IS-associated contigs excludes the highly dynamic
480 regions where ARGs typically reside [6,23,26]. These findings underscore that both host
481 dynamics and plasmid-intrinsic features contribute to the long-term stability and dissemination
482 of plasmids in complex treatment environments.

483 **Methodological considerations and limitations**

484 Our study has several limitations. First, Hi-C captures physical proximity, not definitive
485 biological interaction, and may misassign hosts in dense microbial flocs despite conservative
486 thresholds [23,25,26]. Second, plasmid recovery and clustering are limited by read depth and
487 contig resolution, potentially underrepresenting low-abundance or cryptic plasmids. These
488 factors likely differed across WRRFs and timepoints. As a result, the counts of host-linked
489 plasmid clusters and the apparent network complexity may reflect sampling and recovery
490 differences in addition to biological signal. We reduced these effects by normalizing Hi-C
491 contacts to MAG-mapped reads and plasmid-cluster length, but detection and assembly biases
492 remain. Excluding transposon- and IS-associated contigs further biases results toward more
493 stable elements, possibly missing ARG-carrying plasmids [23]. Third, our study is based on
494 DNA-level data. Without meta-transcriptomics or proteomics, we cannot determine the activity
495 or expression of plasmid-borne genes, limiting functional inference [74]. Lastly, our sampling
496 was limited to three states over three timepoints, which constrains statistical power and the

497 generalizability of observed patterns. Broader spatiotemporal sampling would be needed to fully
498 capture the variability in plasmid–host dynamics across WRRFs.

499 **Conclusions**

500 This study provides new insights into plasmid–host associations in wastewater microbial
501 communities and highlights that certain bacterial groups may play key roles in plasmid
502 maintenance and dissemination. Although wastewater microbial communities are highly diverse,
503 plasmid-associated hosts are constrained to a limited number of bacterial families. By sampling
504 across three WRRFs in three different states, we showed that plasmid host range consistently
505 narrowed from influent to activated sludge, and from activated sludge to effluent, reflecting the
506 effectiveness of different WRRF designs in mitigating plasmid dissemination across treatment
507 stages. These findings are consistent with previous studies suggesting that, although WRRFs
508 have been considered potential “hot spots” for the spread of AMR, WRRFs are very effective at
509 removing plasmids during treatment. Despite their ability to generally remove plasmids during
510 treatment, certain plasmids are persistent across treatment. We found evidence that the hosts of
511 persistent plasmids frequently shift during treatment. These findings suggest possible HGT
512 events, although the underlying mechanisms require further study. Additional evidence for HGT
513 includes the frequent detection of mobility genes and fitness-associated genes on persistent
514 plasmids. Future studies should elucidate the mechanisms underlying plasmid stability in
515 complex communities, which is critical to understanding and mitigating the environmental
516 dissemination of AMR.

517 **List of abbreviations**

518 AMR: Antimicrobial resistance

519 ARG: Antibiotic resistant genes

520 HGT: Horizontal gene transfer

521 ISs: Insertion sequences

522 WRRFs: Water resource recovery facilities

523 MGEs: Mobile genetic elements

524 MAGs: Metagenomic assembled genomes

525 VFs: Virulence factors

526 **Declarations**

527 **Ethics approval and consent to participate**

528 Not applicable

529 **Consent for publication**

530 Not applicable

531 **Availability of data and materials**

532 All sequencing data generated in this study are deposited in the NCBI Sequence Read Archive

533 (SRA) database under the BioProject ID: PRJNA1295499

534 (<https://www.ncbi.nlm.nih.gov/bioproject/PRJNA1295499>). All code needed to reproduce the

535 plasmid clustering and Hi-C plasmid–host linking analyses is available at
536 <https://doi.org/10.17605/OSF.IO/STMU9>. Other relevant information is included in the
537 manuscript and the supplementary files.

538 **Competing interests**

539 The authors declare that they have no competing interests.

540 **Funding**

541 This work was supported by the US–Egypt Science and Technology Joint Fund (NAS Grant
542 G10001728) and under a Cooperative Agreement (W9132T-23-2-0002) with the U.S. Army
543 Corps of Engineers, Engineer Research and Development Center, Construction Engineering
544 Research Laboratory (USACE ERDC-CERL). The funding bodies had no role in the design of
545 the study; in the collection, analysis, and interpretation of data; or in the writing of the
546 manuscript.

547 **Authors' contributions**

548 SZ designed the study, collected samples, conducted computational analyses, and drafted the
549 manuscript. SEP and MAS contributed to sample collection, laboratory processing, and
550 manuscript revision. JDV contributed to data interpretation and manuscript editing. ALS
551 provided funding support and contributed to manuscript revision. LBS supervised the project,
552 contributed to study design, and provided critical feedback. All authors reviewed and approved
553 the final manuscript and agreed to be accountable for all aspects of the work.

554 **Acknowledgements**

555 We thank the wastewater utilities for providing access to sampling sites. We also thank the
556 participating wastewater treatment facilities for enabling sample collection.

557 **Reference**

- 558 1. Bennett PM. Plasmid encoded antibiotic resistance: acquisition and transfer of antibiotic
559 resistance genes in bacteria. *Br J Pharmacol.* 2008;153:S347–57.
- 560 2. Smalla K, Jechalke S, Top EM. Plasmid Detection, Characterization, and Ecology. *Microbiol*
561 *Spectr.* 2015;3:10.1128/microbiolspec.plas-0038–2014.
- 562 3. Coluzzi C, Garcillán-Barcia MP, de la Cruz F, Rocha EPC. Evolution of Plasmid Mobility:
563 Origin and Fate of Conjugative and Nonconjugative Plasmids. *Mol Biol Evol.* 2022;39:msac115.
- 564 4. Barlow M. What antimicrobial resistance has taught us about horizontal gene transfer.
565 *Methods Mol Biol Clifton NJ.* 2009;532:397–411.
- 566 5. Smillie C, Garcillán-Barcia MP, Francia MV, Rocha EPC, de la Cruz F. Mobility of Plasmids.
567 *Microbiol Mol Biol Rev.* 2010;74:434–52.
- 568 6. Che Y, Yang Y, Xu X, Břinda K, Polz MF, Hanage WP, et al. Conjugative plasmids interact
569 with insertion sequences to shape the horizontal transfer of antimicrobial resistance genes. *Proc*
570 *Natl Acad Sci.* 2021;118:e2008731118.
- 571 7. Sünderhauf D, Klümper U, Gaze WH, Westra ER, van Houte S. Interspecific competition can
572 drive plasmid loss from a focal species in a microbial community. *ISME J.* 2023;17:1765–73.
- 573 8. Benz F, Hall AR. Host-specific plasmid evolution explains the variable spread of clinical
574 antibiotic-resistance plasmids. *Proc Natl Acad Sci.* 2023;120:e2212147120.
- 575 9. Bottery MJ. Ecological dynamics of plasmid transfer and persistence in microbial
576 communities. *Curr Opin Microbiol.* 2022;68:102152.
- 577 10. Li L-G, Zhang T. Plasmid-mediated antibiotic resistance gene transfer under environmental
578 stresses: Insights from laboratory-based studies. *Sci Total Environ.* 2023;887:163870.
- 579 11. van Elsas JD, Bailey MJ. The ecology of transfer of mobile genetic elements. *FEMS*
580 *Microbiol Ecol.* 2002;42:187–97.
- 581 12. Cook LCC, Dunny GM. The influence of biofilms in the biology of plasmids. *Microbiol*
582 *Spectr.* 2014;2:0012.
- 583 13. Wang S, Li W, Xi B, Cao L, Huang C. Mechanisms and influencing factors of horizontal
584 gene transfer in composting system: A review. *Sci Total Environ.* 2024;955:177017.

- 585 14. Schlüter A, Heuer H, Szczepanowski R, Forney LJ, Thomas CM, Pühler A, et al. The 64508
586 bp IncP-1 β antibiotic multiresistance plasmid pB10 isolated from a waste-water treatment plant
587 provides evidence for recombination between members of different branches of the IncP-1 β
588 group. *Microbiology*. 2003;149:3139–53.
- 589 15. Schlüter A, Szczepanowski R, Pühler A, Top EM. Genomics of IncP-1 antibiotic resistance
590 plasmids isolated from wastewater treatment plants provides evidence for a widely accessible
591 drug resistance gene pool. *FEMS Microbiol Rev*. 2007;31:449–77.
- 592 16. Mosaka TBM, Unuofin JO, Daramola MO, Tizaoui C, Iwarere SA. Inactivation of antibiotic-
593 resistant bacteria and antibiotic-resistance genes in wastewater streams: Current challenges and
594 future perspectives. *Front Microbiol* [Internet]. 2023 [cited 2025 Mar 5];13. Available from:
595 <https://www.frontiersin.org/journals/microbiology/articles/10.3389/fmicb.2022.1100102/full>
- 596 17. Zhang S, Wang Y, Lu J, Yu Z, Song H, Bond PL, et al. Chlorine disinfection facilitates
597 natural transformation through ROS-mediated oxidative stress. *ISME J*. 2021;15:2969–85.
- 598 18. Lopatkin AJ, Meredith HR, Srimani JK, Pfeiffer C, Durrett R, You L. Persistence and
599 reversal of plasmid-mediated antibiotic resistance. *Nat Commun*. 2017;8:1689.
- 600 19. Alonso-del Valle A, León-Sampedro R, Rodríguez-Beltrán J, DelaFuente J, Hernández-
601 García M, Ruiz-Garbajosa P, et al. Variability of plasmid fitness effects contributes to plasmid
602 persistence in bacterial communities. *Nat Commun*. 2021;12:2653.
- 603 20. Pallares-Vega R, Macedo G, Brouwer MSM, Hernandez Leal L, van der Maas P, van
604 Loosdrecht MCM, et al. Temperature and Nutrient Limitations Decrease Transfer of Conjugative
605 IncP-1 Plasmid pKJK5 to Wild *Escherichia coli* Strains. *Front Microbiol*. 2021;12:656250.
- 606 21. Ma J, Sun H, Li B, Wu B, Zhang X, Ye L. Horizontal transfer potential of antibiotic
607 resistance genes in wastewater treatment plants unraveled by microfluidic-based mini-
608 metagenomics. *J Hazard Mater*. 2024;465:133493.
- 609 22. Zhang Y, Xue B, Mao Y, Chen X, Yan W, Wang Y, et al. High-throughput single-cell
610 sequencing of activated sludge microbiome. *Environ Sci Ecotechnology*. 2025;23:100493.
- 611 23. Risely A, Newbury A, Stalder T, Simmons BI, Top EM, Buckling A, et al. Host- plasmid
612 network structure in wastewater is linked to antimicrobial resistance genes. *Nat Commun*.
613 2024;15:555.
- 614 24. McCorison CB, Kim T, Donato JJ, LaPara TM. Proximity-Ligation Metagenomic Sequence
615 Analysis Reveals That the Antibiotic Resistome Makes Significant Transitions During Municipal
616 Wastewater Treatment. *Environ Microbiol*. 2025;27:e70036.
- 617 25. Stalder T, Press MO, Sullivan S, Liachko I, Top EM. Linking the resistome and plasmidome
618 to the microbiome. *ISME J*. 2019;13:2437–46.

- 619 26. McCallum GE, Rossiter AE, Quraishi MN, Iqbal TH, Kuehne SA, van Schaik W. Noise
620 reduction strategies in metagenomic chromosome confirmation capture to link antibiotic
621 resistance genes to microbial hosts. *Microb Genomics*. 2023;9:001030.
- 622 27. Li D, Liu C-M, Luo R, Sadakane K, Lam T-W. MEGAHIT: an ultra-fast single-node solution
623 for large and complex metagenomics assembly via succinct de Bruijn graph. *Bioinformatics*.
624 2015;31:1674–6.
- 625 28. Langmead B, Salzberg SL. Fast gapped-read alignment with Bowtie 2. *Nat Methods*.
626 2012;9:357–9.
- 627 29. Li H, Handsaker B, Wysoker A, Fennell T, Ruan J, Homer N, et al. The Sequence
628 Alignment/Map format and SAMtools. *Bioinformatics*. 2009;25:2078–9.
- 629 30. Li H. Aligning sequence reads, clone sequences and assembly contigs with BWA-MEM
630 [Internet]. arXiv.org. 2013 [cited 2025 Jun 16]. Available from:
631 <https://arxiv.org/abs/1303.3997v2>
- 632 31. Du Y, Sun F. MetaCC allows scalable and integrative analyses of both long-read and short-
633 read metagenomic Hi-C data. *Nat Commun*. 2023;14:6231.
- 634 32. Press M, Stalder T, Genomics P. Arg-Plasmid-Genome connections from Hi-C. 2018 [cited
635 2025 Jun 16]; Available from: <https://osf.io/ezb8j/>
- 636 33. Seemann T. Prokka: rapid prokaryotic genome annotation. *Bioinformatics*. 2014;30:2068–9.
- 637 34. Chaumeil P-A, Mussig AJ, Hugenholtz P, Parks DH. GTDB-Tk: a toolkit to classify genomes
638 with the Genome Taxonomy Database. *Bioinformatics*. 2020;36:1925–7.
- 639 35. Parks DH, Imelfort M, Skennerton CT, Hugenholtz P, Tyson GW. CheckM: assessing the
640 quality of microbial genomes recovered from isolates, single cells, and metagenomes. *Genome*
641 *Res*. 2015;25:1043–55.
- 642 36. Camargo AP, Roux S, Schulz F, Babinski M, Xu Y, Hu B, et al. Identification of mobile
643 genetic elements with geNomad. *Nat Biotechnol*. 2024;42:1303–12.
- 644 37. Hyatt D, Chen G-L, LoCascio PF, Land ML, Larimer FW, Hauser LJ. Prodigal: prokaryotic
645 gene recognition and translation initiation site identification. *BMC Bioinformatics*. 2010;11:119.
- 646 38. Siguier P, Perochon J, Lestrade L, Mahillon J, Chandler M. ISfinder: the reference centre for
647 bacterial insertion sequences. *Nucleic Acids Res*. 2006;34:D32-36.
- 648 39. Ross K, Varani AM, Snesrud E, Huang H, Alvarenga DO, Zhang J, et al. TnCentral: a
649 Prokaryotic Transposable Element Database and Web Portal for Transposon Analysis. *mBio*.
650 12:e02060-21.

- 651 40. The igraph software package for complex network research | BibSonomy [Internet]. [cited
652 2025 Jun 16]. Available from:
653 <https://www.bibsonomy.org/bibtex/bb49a4a77b42229a427fec316e9fe515>
- 654 41. Dewan I, Uecker H. Is the distribution of plasmid lengths bimodal? *Plasmid*. 2024;129–
655 130:102721.
- 656 42. Finks SS, Martiny JBH. Plasmid-Encoded Traits Vary across Environments. *mBio*.
657 14:e03191-22.
- 658 43. Robertson J, Nash JHE. MOB-suite: software tools for clustering, reconstruction and typing
659 of plasmids from draft assemblies. *Microb Genomics*. 2018;4:e000206.
- 660 44. Chen L, Yang J, Yu J, Yao Z, Sun L, Shen Y, et al. VFDB: a reference database for bacterial
661 virulence factors. *Nucleic Acids Res*. 2005;33:D325-328.
- 662 45. Feldgarden M, Brover V, Gonzalez-Escalona N, Frye JG, Haendiges J, Haft DH, et al.
663 AMRFinderPlus and the Reference Gene Catalog facilitate examination of the genomic links
664 among antimicrobial resistance, stress response, and virulence. *Sci Rep*. 2021;11:12728.
- 665 46. Oksanen J, Simpson GL, Blanchet FG, Kindt R, Legendre P, Minchin PR, et al. vegan:
666 Community Ecology Package [Internet]. 2025 [cited 2025 Jun 16]. Available from: [https://cran.r-](https://cran.r-project.org/web/packages/vegan/index.html)
667 [project.org/web/packages/vegan/index.html](https://cran.r-project.org/web/packages/vegan/index.html)
- 668 47. McKight PE, Najab J. Kruskal-Wallis Test. *Corsini Encycl Psychol* [Internet]. John Wiley &
669 Sons, Ltd; 2010 [cited 2025 Jun 16]. p. 1–1. Available from:
670 <https://onlinelibrary.wiley.com/doi/abs/10.1002/9780470479216.corpsy0491>
- 671 48. Kassambara A. ggpubr: “ggplot2” Based Publication Ready Plots [Internet]. 2023 [cited 2025
672 Jun 16]. Available from: <https://cran.r-project.org/web/packages/ggpubr/index.html>
- 673 49. Sen D, Van der Auwera GA, Rogers LM, Thomas CM, Brown CJ, Top EM. Broad-Host-
674 Range Plasmids from Agricultural Soils Have IncP-1 Backbones with Diverse Accessory Genes.
675 *Appl Environ Microbiol*. 2011;77:7975–83.
- 676 50. Brown CJ, Sen D, Yano H, Bauer ML, Rogers LM, Van der Auwera GA, et al. Diverse
677 Broad-Host-Range Plasmids from Freshwater Carry Few Accessory Genes. *Appl Environ*
678 *Microbiol*. 2013;79:7684–95.
- 679 51. Carrión VJ, Cordovez V, Tyc O, Etalo DW, de Bruijn I, de Jager VCL, et al. Involvement of
680 Burkholderiaceae and sulfurous volatiles in disease-suppressive soils. *ISME J*. 2018;12:2307–21.
- 681 52. DeShazer D. A novel contact-independent T6SS that maintains redox homeostasis via Zn²⁺
682 and Mn²⁺ acquisition is conserved in the *Burkholderia pseudomallei* complex. *Microbiol Res*.
683 2019;226:48–54.

- 684 53. Bayer B, Saito MA, McIlvin MR, Lückner S, Moran DM, Lankiewicz TS, et al. Metabolic
685 versatility of the nitrite-oxidizing bacterium *Nitrospira marina* and its proteomic response to
686 oxygen-limited conditions. *ISME J.* 2021;15:1025–39.
- 687 54. Petri RM, Schwaiger T, Penner GB, Beauchemin KA, Forster RJ, McKinnon JJ, et al.
688 Changes in the Rumen Epimural Bacterial Diversity of Beef Cattle as Affected by Diet and
689 Induced Ruminal Acidosis. *Appl Environ Microbiol.* 2013;79:3744–55.
- 690 55. Jordt H, Stalder T, Kosterlitz O, Ponciano JM, Top EM, Kerr B. Coevolution of host–plasmid
691 pairs facilitates the emergence of novel multidrug resistance. *Nat Ecol Evol.* 2020;4:863–9.
- 692 56. Benz F, Huisman JS, Bakkeren E, Herter JA, Stadler T, Ackermann M, et al. Plasmid- and
693 strain-specific factors drive variation in ESBL-plasmid spread in vitro and in vivo. *ISME J.*
694 2021;15:862–78.
- 695 57. Pei R, Gunsch CK. Plasmid Conjugation in an Activated Sludge Microbial Community.
696 *Environ Eng Sci.* 2009;26:825–31.
- 697 58. Li L, Dechesne A, Madsen JS, Nesme J, Sørensen SJ, Smets BF. Plasmids persist in a
698 microbial community by providing fitness benefit to multiple phylotypes. *ISME J.*
699 2020;14:1170–81.
- 700 59. Król JE, Nguyen HD, Rogers LM, Beyenal H, Krone SM, Top EM. Increased Transfer of a
701 Multidrug Resistance Plasmid in *Escherichia coli* Biofilms at the Air-Liquid Interface. *Appl*
702 *Environ Microbiol.* 2011;77:5079–88.
- 703 60. Qiu T, Shen L, Guo Y, Gao M, Gao H, Li Y, et al. Impact of aeration rate on the transfer
704 range of antibiotic-resistant plasmids during manure composting. *Environ Pollut.*
705 2024;361:124851.
- 706 61. Qin L, Wang D, Zhang Z, Li X, Chai G, Lin Y, et al. Impact of Dissolved Oxygen on the
707 Performance and Microbial Dynamics in Side-Stream Activated Sludge Hydrolysis Process.
708 *Water.* 2023;15:1977.
- 709 62. Yadav TC, Khardenavis AA, Kapley A. Shifts in microbial community in response to
710 dissolved oxygen levels in activated sludge. *Bioresour Technol.* 2014;165:257–64.
- 711 63. Riisgaard-Jensen M, Dottorini G, Nierychlo M, Nielsen PH. Primary settling changes the
712 microbial community of influent wastewater to wastewater treatment plants. *Water Res.*
713 2023;244:120495.
- 714 64. Zhou S, Yang Z, Zhang S, Gao Y, Tang Z, Duan Y, et al. Metagenomic insights into the
715 distribution, mobility, and hosts of extracellular antibiotic resistance genes in activated sludge
716 under starvation stress. *Water Res.* 2023;236:119953.
- 717 65. Jong M-C, Harwood CR, Blackburn A, Snape JR, Graham DW. Impact of Redox Conditions
718 on Antibiotic Resistance Conjugative Gene Transfer Frequency and Plasmid Fate in Wastewater
719 Ecosystems. *Environ Sci Technol.* 2020;54:14984–93.

- 720 66. Kempf I, Le Devendec L, Lucas P, Druilhe C, Pourcher A-M. Impact of mesophilic anaerobic
721 digestion and post-treatment of digestates on the transfer of conjugative antimicrobial resistance
722 plasmids. *Waste Manag.* 2022;152:1–5.
- 723 67. Wang Y, Wang Y, Shang J, Wang L, Li Y, Wang Z, et al. Redox gradients drive microbial
724 community assembly patterns and molecular ecological networks in the hyporheic zone of
725 effluent-dominated rivers. *Water Res.* 2024;248:120900.
- 726 68. Zhang Y, Mao Q, Su Y, Zhang H, Liu H, Fu B, et al. Thermophilic rather than mesophilic
727 sludge anaerobic digesters possess lower antibiotic resistant genes abundance. *Bioresour*
728 *Technol.* 2021;329:124924.
- 729 69. Brown CL, Maile-Moskowitz A, Lopatkin AJ, Xia K, Logan LK, Davis BC, et al. Selection
730 and horizontal gene transfer underlie microdiversity-level heterogeneity in resistance gene fate
731 during wastewater treatment. *Nat Commun.* 2024;15:5412.
- 732 70. Jäger T, Hembach N, Elpers C, Wieland A, Alexander J, Hiller C, et al. Reduction of
733 Antibiotic Resistant Bacteria During Conventional and Advanced Wastewater Treatment, and the
734 Disseminated Loads Released to the Environment. *Front Microbiol* [Internet]. 2018 [cited 2025
735 Apr 3];9. Available from:
736 <https://www.frontiersin.org/journals/microbiology/articles/10.3389/fmicb.2018.02599/full>
- 737 71. Fang G-Y, Liu X-Q, Jiang Y-J, Mu X-J, Huang B-W. Horizontal gene transfer in activated
738 sludge enhances microbial antimicrobial resistance and virulence. *Sci Total Environ.*
739 2024;912:168908.
- 740 72. An X-L, Chen Q-L, Zhu D, Zhu Y-G, Gillings MR, Su J-Q. Impact of Wastewater Treatment
741 on the Prevalence of Integrons and the Genetic Diversity of Integron Gene Cassettes. *Appl*
742 *Environ Microbiol.* 2018;84:e02766-17.
- 743 73. Zorea A, Pellow D, Levin L, Pilosof S, Friedman J, Shamir R, et al. Plasmids in the human
744 gut reveal neutral dispersal and recombination that is overpowered by inflammatory diseases.
745 *Nat Commun.* 2024;15:3147.
- 746 74. Bashiardes S, Zilberman-Schapira G, Elinav E. Use of Metatranscriptomics in Microbiome
747 Research. *Bioinforma Biol Insights.* 2016;10:19–25.
- 748